Asian Journal of Chemistry; Vol. 35, No. 5 (2023), 1243-1249

ASIAN JOURNAL OF CHEMISTRY

https://doi.org/10.14233/ajchem.2023.27786

Electrochemical Sensing of Dopamine at Biogenic Gold Nanoparticles Interface

Sachin J. Kamble[1,*], Anita K. Tawade[2], Kiran D. Pawar[2], Jayashri B. Kamble[3], Prakash D. Kamble[4], Vikram B. More[5], Nitin M. Naik[5], Valmiki B. Koli[6], Ganesh S. Kamble[7] and Jaykumar M. Patil[8]

[1]Department of Chemistry, Sanjay Ghodawat Polytechnic, Atigre-416118, India
[2]School of Nanoscience and Nanotechnology, Shivaji University, Kolhapur-416004, India
[3]Department of Chemistry, Shivaji University, Kolhapur-416004, India
[4]Department of Chemistry, Balasaheb Desai College, Patan-415206, India
[5]Department of Biochemistry, Shivaji University, Kolhapur-416004, India
[6]Deaprtment of Physics, National Dong-Hwa University, Shou-Feng 97401, Taiwan
[7]Department of Engineering Chemistry, Kolhapur Institute of Technology's College of Engineering (Autonomous), Kolhapur-416004, India
[8]Department of Chemistry, D.K.T.E. Society's Textiles and Engineering Institute, Ichalkaranji-416115, India

*Corresponding author: E-mail: sachin.kamble305@gmail.com

Received: 14 March 2023; *Accepted*: 17 April 2023; *Published online*: 28 April 2023; AJC-21235

A simple biogenic synthetic route for the development of gold nanoparticles (Au NPs) from the fresh pods of *Lablab purpureus* was carried out. Further, Au NPs modified electrode employed for the selective sensing of dopamine. The stability, surface morphologies, microstructure and elemental compositions of the nanoparticles were probed by dynamic light scattering (DLS) with zeta potential, transmission electron microscopy (TEM), energy dispersive X-ray diffraction (EDX) and X-ray diffraction (XRD). The electrochemical features of dopamine at Au NPs modified glassy carbon electrodes (GCEs) was investigated in 0.1 M phosphate buffer solution (pH 7.4) by cyclic voltammetry (CV) and differential pulse voltammetry (DPV). Gold nanoparticles modified GCEs in comparison with bare electrodes shows the significant catalytic activity towards dopamine from CV and DPV with limit of detection 5.9 nM and 7.7 nM, respectively. Additionally, the peak current response of dopamine does not interfered with the coexistence of ascorbic acid, uric acid and glucose.

Keywords: Dopamine, Gold nanoparticles, *Lablab purpureus*, Cyclic voltammetry, Electrochemical sensor.

INTRODUCTION

Dopamine is considered as significant catecholamine neurotransmitter, which plays crucial role in the nervous system [1,2]. For healthy human being an acceptable concentrations of dopamine in urine and blood serum are 0.1 M and 0.5-25 nM, respectively. However, the abnormal concentration and dopamine deficiency can results mental disorder with severe conditions such as Parkinson's disease and Schizophrenia [3,4]. Hence, monitoring of biological fluids for early disease detection has become an important factor [5,6]. Thus, it is necessary to develop technologies with high selectivity, more sensitive, for the effective detection of dopamine in biological fluids. So far traditionally approaches have been employed for sensing of dopamine such as HPLC [7], fluorescence [8], surface plasmon resonance [9], colorimetric [10] and electrochemical techniques [11].

Among all above mentioned methods, electrochemical techniques cyclic voltammetry (CV) and differential pulse voltammetry (DPV) are commonly utilized due to its simplicity and high sensitivity [12]. The unmodified electrode fails to illustrate complete and neat separation of electrochemical signals from the mixture of biological fluids' (dopamine, uric acid and ascorbic acid), this is due to the cohabitation of biomolecules [13]. Therefore, recognition of such mixed biomolecules is quite difficult due to their identical electrochemical features [14]. Gold nanoparticles (Au NPs) have recently drawn an increasing attention of many researchers in the field of sensors especially biosensor attributed to its novel chemical, optical and physical properties [15,16]. Some of its unique properties are high effective surface-to-volume ratio, excellent electrical and heat conductivity and strong absorption in the visible and near infrared wavelength region (380-750 nm). Gold nanoparticles (Au NPs) also exhibit

This is an open access journal, and articles are distributed under the terms of the Attribution 4.0 International (CC BY 4.0) License. This license lets others distribute, remix, tweak, and build upon your work, even commercially, as long as they credit the author for the original creation. You must give appropriate credit, provide a link to the license, and indicate if changes were made.

high chemical stability and inertness under physiological conditions as well as possesses excellent electro-catalytic properties. All these properties make Au NPs an attractive material in multifunctional applications especially in electrochemical and biological devices. More interestingly, the properties of Au NPs can be controlled by tuning the shape and size of gold nanoparticles [17]. Herein, the biogenic synthesis of Au NPs from fresh pods of *Lablab purpureus* was carried out. Furthermore, Au NPs was utilized for modification of GCE and the design Au NPs/GCE was used as a working electrode for the detection of dopamine.

EXPERIMENTAL

Chloroauric acid tetrahydrate ($HAuCl_4 \cdot 4H_20$, ≥ 99.9%; HiMedia, India), potassium dihydrogen orthophosphate (KH_2PO_4), dipotassium hydrogen phosphate (K_2HPO_4) were obtained from (SD Fine-Chem Ltd.) All the chemicals were used as received without further purification and their solutions were prepared in Milli-Q water. Glassy carbon electrodes (GCEs), C110 of 3 mm diameter were used as working electrodes, counter electrode platinum (Pt) and a reference electrode was Ag/AgCl. All the electrochemical experiments were performed with the three-electrode system (Autolab Metrohm PGSTAT 302N).

Preparation of Lablab Purpureus pods extract: Fresh pods of Lablab Purpureus were collected from a local village Sajani, Dist. Kolhapur, (Latitude: 16.7163º N and Longitude: 74.3954º E). Pods were washed thoroughly under running tap water to remove dirt and other foreign particles attached to it, followed by double distilled water twice. These pods were weighed 10 g accurately, chopped into small pieces and then transferred to 250 mL glass beaker containing 100 mL of double distilled water. It was then stirred well using a clean glass rod and then this mixture was boiled for 15 min at 80 ºC. The extract formed thus was then filtered using Whatmann filter paper No. 1 and then filtrate was stored at 4 ºC for further use.

Synthesis of gold nanoparticles: To synthesize gold nanoparticles (Au NPs), 10 mL freshly obtained pod extract was added to a 100 mL of 0.001 M $HAuCl_4 \cdot 4H_2O$ solution dropwise with constant stirring. A transparent light yellow colour of reaction mixture was changed to purple colour, which primarily indicates the formation of Au NPs. This reaction was monitored by UV-Vis spectroscopy.

Characterization: The biogenic synthesized Au NPs were characterized by using various spectroscopic and imaging techniques. Fourier transform infrared (FTIR) spectroscopy (Shimadzu, Japan) analysis has confirmed the functional group (s) responsible for the biosynthesis of Au NPs. Elemental compositions was detected by using energy dispersive X-ray (EDS) spectrometer with x-act with INCA® and Aztec® EDS analysis software (Oxford Instruments, UK). The crystalline nature of Au NPs was studied by recording X-ray powder diffraction (XRD) pattern on X-ray powder diffractometer (Bruker AXS Analytical Instruments Pvt. Ltd. Germany).

RESULTS AND DISCUSSION

A simpler one-step and greener method for the synthesis of gold nanoparticles (Au NPs) using the fresh pods of *Lablab purpureus* was carried out. Furthermore, the morphological studies of synthesized gold nanoparticles using TEM images revealed that approximately 90% of the nanoparticles were spherical and monodisperse. Upon mixing *Lablab purpureus* pod extract with aqueous chloroauric acid, the solution colour transmuted from pale yellow to purple, indicating the successful formation of Au NPs. This visible purple colour was due to the localized surface plasmon resonance (SPR) of Au NPs with a diameter less than 50 nm [18,19]. The widely accepted proposed mechanism for the synthesis of Au NPs involves a phytochemical reaction in which complex reducing compounds present in plant extract, such as antioxidants, enzymes and phenolic moieties, reduce gold cations (Au^{3+}) into Au NPs (Au^0) [20-23]. The hypothetical reduction of $HAuCl_4 \cdot 4H_2O$ is driven by the presence of the phytochemicals to form zero-valent gold, which will subsequently lead to the agglomeration of gold atoms to nanoparticles, which are finally stabilized by the phytochemicals itself. Plants including *Lablab purpureus* contain a complex biological network of antioxidant metabolites and enzymes that work collectively to prevent oxidative damage to cellular components [24]. Earlier publications showed that plant extracts contain biomolecules including polyphenols, flavonoids, sterols, ascorbic acid, triterpenes, alkaloids, alcoholic compounds, saponins, β-phenylethylamines, polysaccharides, glucose, fructose and proteins/enzymes, which could act as reducing agents for metal cations, leading to the formation of Au NPs [25]. It also seems probable that glucose and ascorbate can reduce gold ions to form nanoparticles at elevated temperatures [26]. Proteins, enzymes, phenolics and other chemical compounds within the pod extracts can reduce gold salts and provide exquisite tenacity toward the agglomeration of the formed nanoparticles. The biogenic synthesized Au NPs exhibited an excellent colloidal stability and surface capping that might be because of phytochemicals present in the extract.

Characterization of biogenic Au NPs

UV-VIS studies: A typical absorbance peak at 525 nm for Au NPs has been confirmed the formation of Au NPs. Furthermore, a change in colour of the extract from pale yellow to purple indicates successful formation of Au NPs. A intensity of the colour goes on increasing as the reaction proceeds. The typical surface plasmon peak in the range of 520-540 nm with peak maximum in the range 527-535 nm in the UV-visible spectrum (Fig. 1) confirms formation of Au NPs in the solution. The completion of this reaction is also confirmed by this technique as the surface plasmon peak remains stable after 5 min of time.

XRD studies: XRD pattern of the biogenic synthesis of Au NPs has revealed the three important peaks present in the 2θ range (Fig. 2). The diffraction peaks of 39.2º relates to (111), 45.2º relates to (200) and 65.5º relates to (220) facets of the face centered cubic (FCC) crystal lattice. These values agreed with reported values for similar gold nanostructures [27] and also matched its planes and FCC structure with Au NPs prepared by other reported works [28-30]. The peaks obtained are consistent with and matched Joint Committee on Powder Diffraction Standards (JCPDS) card No. 04-0784.

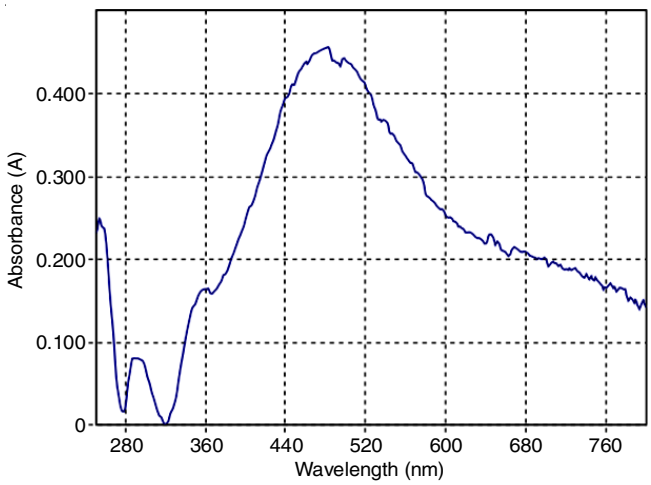

Fig. 1. UV-visible absorption spectrum of reaction mixture

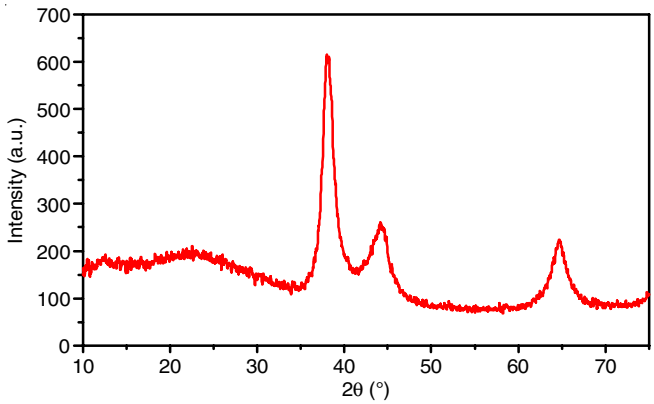

Fig. 2. X-ray diffraction spectrum of biosynthesized gold nanoparticles

FT-IR studies: The FTIR spectra of neat *L. purpureus* pod extract and synthesized Au NPs (Fig. 3a-b) were recorded to analyze the functional groups of biomolecules that could have acted as reducing and capping agents in the bioreduction. A prominent peak at 3268 cm^{-1} in the IR spectra of pod extract and Au NPs was attributed to O-H stretching of alcohol or phenol, whereas peaks observed at 2358 cm^{-1} in extract and 2105 cm^{-1} in IR spectra of Au NPs are due to the C≡C stretching vibrations of carboxylic acid. The bands at 1634 cm^{-1} that could be attributed to the stretching vibrations of aromatic C=C observed in both spectra. The other peaks observed at 1373 and 748 cm^{-1} in extract and Au NPs correspond to the aromatic stretching of C=C of alkenes and C-N stretching vibration of amine, respectively. The comparison of IR spectra of neat extract and Au NPs shows that the peak observed at 2358 cm^{-1} corresponding to the carboxylic acid, which could be responsible for the bioreduction and capping mechanisms during the biogenic Au NPs synthesis.

Morphological studies: The shape, size and dispersity of Au NPs were studied using TEM images (Fig. 4) and particle size analysis. This showed that biogenic Au NPs were monodispersed with no aggregates, spherical in shape with size ranging between 10 and 15 nm. The crystalline structure of Au NPs indicated by XRD pattern was further confirmed by SAED, which showed circular white spots that were indexed to face centered cubic structure of Au NPs.

The SAED pattern (Fig. 5a) showed the different phase arrangement, which displayed five circular bright rings correlated to the (111), (200) and (220) planes. This SAED pattern along with XRD analysis clearly indicated that biogenic Au NPs were crystalline in nature. The synthesis of Au NPs has been validated by the EDAX spectra (Fig. 5b) of synthesised Au NPs, which displayed a strong Au signal in the form of a sharp peak at 2.0 keV. Along with this, many peaks of C, O, Mg, Cl and K, were also observed these were originated from surface bound biomolecules.

Cyclic voltammetry studies: In order to evaluate the efficiency of sensor, CV was performed for the determination of dopamine using Au NPs modified electrode 0.1 M PBS. Fig. 6a depicts the CV response of dopamine oxidation at Au NPs modified electrode for the successive additions of dopamine (0 M to 39.5 nM) in 0.1 M PBS (pH 7.4). It can be seen that the oxidation peak current was significantly increased with increasing the concentrations of dopamine. The oxidation of dopamine the anodic peak current was liner dependent over the concentrations of 0 M to 39.5 nM as shown in Fig. 6b-c. The linear regression equation is expressed as I_{pa} (nM) = 182.2 [DOPA] (mol L^{-1}) + 4 × 10^{-6} (R^2 = 0.99). The calculated limit

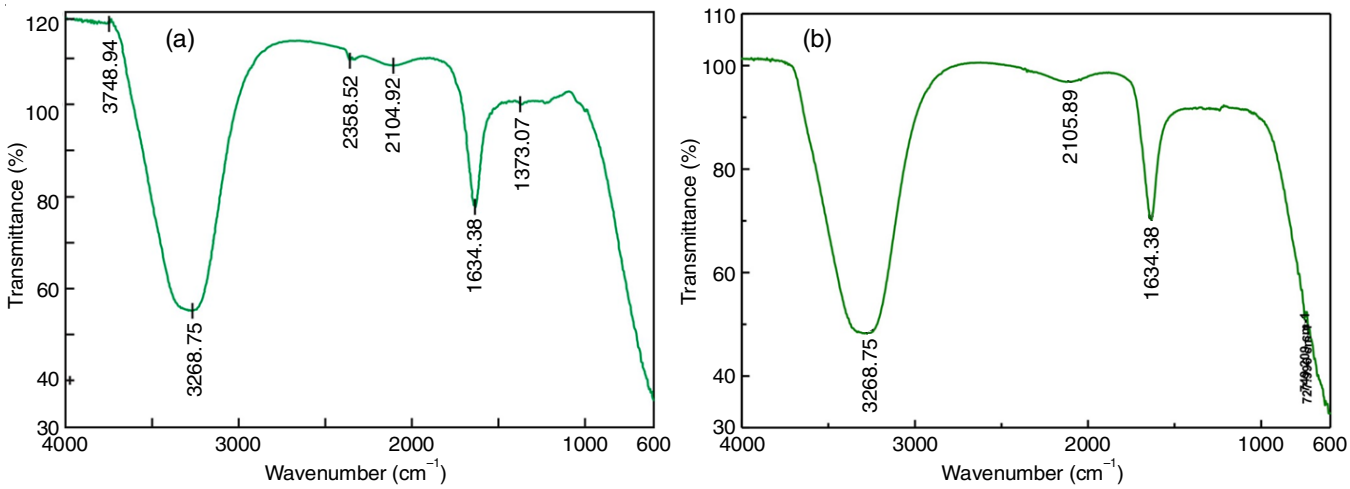

Fig. 3. FTIR spectrum of (a) pod extract and (b) biogenic Au NPs

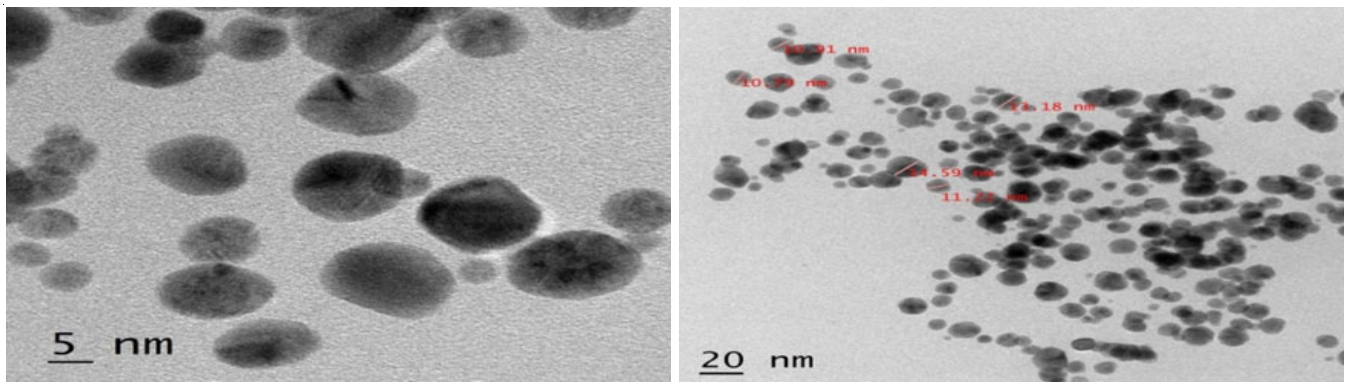

Fig. 4. Transmission electron microscope (TEM) images at 5 nm and 20 nm scales

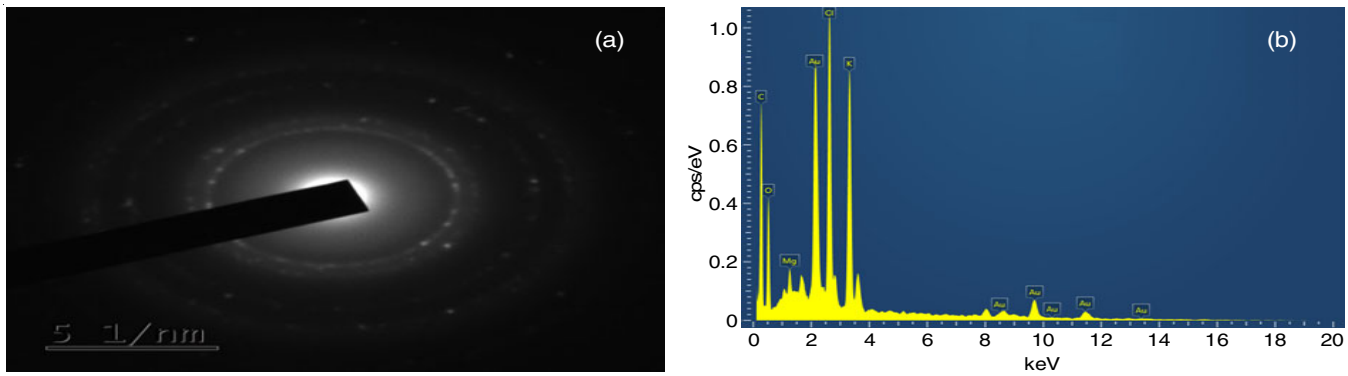

Fig. 5. (a) SAED pattern of biogenic Au_NPs and (b) energy dispersive X-ray (EDAX) spectra of Au NPs

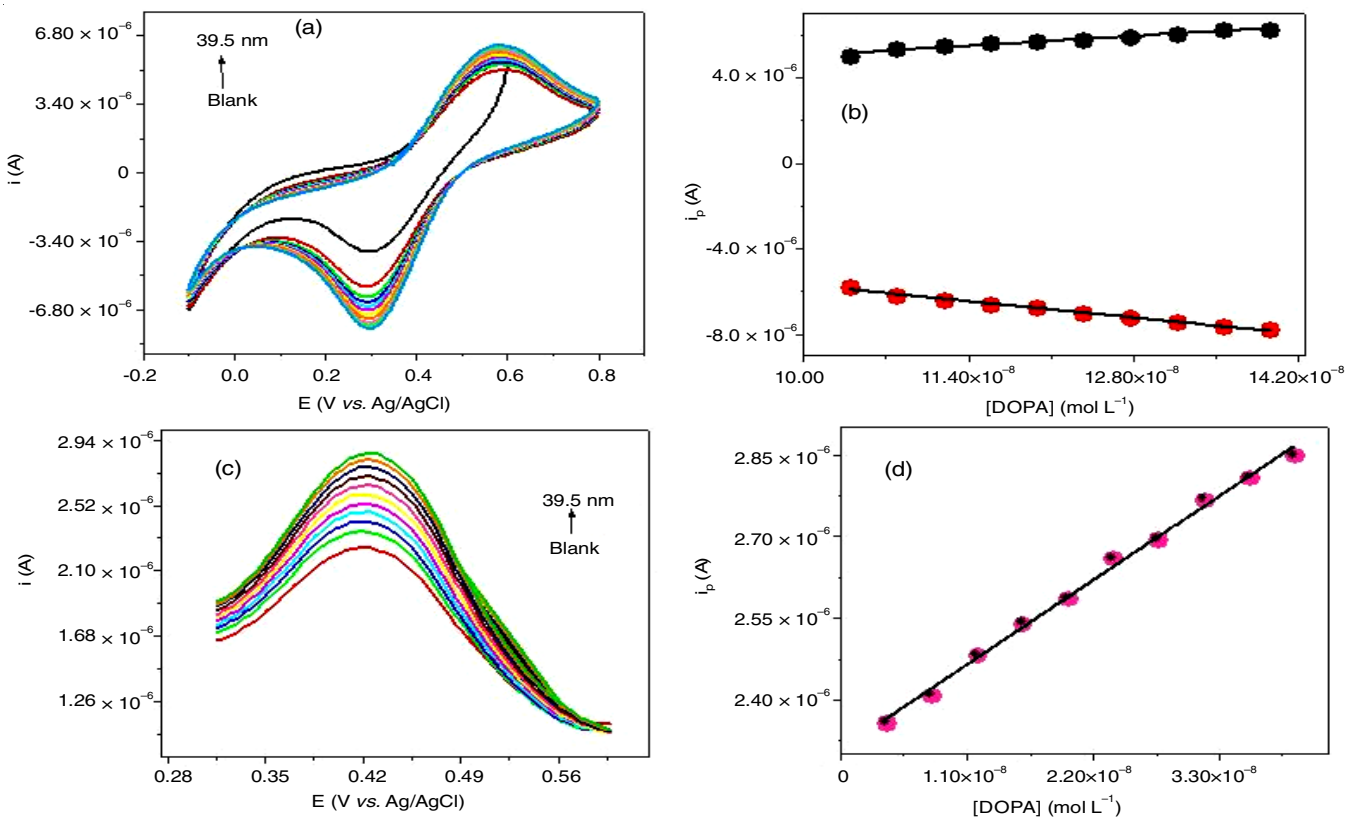

Fig. 6. (a) CV response for Au NPs modified GCEs towards the detection dopamine in various concentration 0 M to 39.5 nM, 0.1 M PBS (pH 7.4) and scan rate of 50 mV/s; (b) calibration plot of Au NPs/GCE with successive addition of dopamine in a solution; (c) DPV response for Au NPs modified GCEs towards the detection dopamine in various concentration 0 M to 39.5 nM, 0.1 M PBS and scan rate of 50 mV/s; (d) calibration plot of Au NPs/GCE with successive addition of dopamine in a solution

of detection (LOD) was achieved to be 5.94 nM based on signa to noise ratio (S/N = 3) with a sensitivity of 2024 AM^{-1} cm^{-2}.

The DPV was performed with successive addition of dopamine to 0.1 M phosphate buffer solution at 0.1 M PBS (pH 7.4). On plotting the calibration curve, the linear variation of anodic current with concentration was observed (Fig. 6d). The overall performance of the sensor was better in the range of 0 M to 39.5 nM with a sensitivity of 173 AM^{-1} cm^{-2} with a regression coefficient value (R^2 value) of 0.99. Limit of detection (LOD) was determined to be 7.46 nM based on the formula 3SD/sensitivity (where SD = standard deviation and sensitivity = slope of calibration plot).

The effect of scan rate was investigated towards the oxidation dopamine using the Au NPs/GCE modified electrode in 0.1 M PBS (pH 7.4) at different scan rates ranging from 10-100 mV/s as shown in Fig. 7a. With increasing the scan rates (10 to 100 mV/s), the oxidation peak current of dopamine was increased with a systematic redox pairs. Fig. 7b showed the linear relationship between the scan rate and the peak current of dopamine with a correlation coefficient of 0.99 and 0.99 for anodic (I_{pa}) and cathodic (I_{pc}) peak currents, respectively, which suggest that the electro-oxidation of dopamine was controlled by adsorption-controlled electrochemical process on the electrode surface [31,32]. In addition, the protonation of dopamine oxidation at different pH solutions using Au NPs modified electrode was studied by CV and the results are shown in Fig. 7c. It can be seen that the higher oxidation peak current was observed in pH 7.4, while increasing or decreasing the solution pH (6 and 8) peak current was gradually decreased and the peak potential was shift towards positive and negative directions. Hence, the pH 7.4 is an optimum for the electro-oxidation of dopamine at Au NPs modified GCE.

It is well known that uric acid, ascorbic acid and other amino acid, caffeine, L alanine, L-phenylalanine are the potential biological molecules, which are commonly interfering with dopamine detection. Hence, we have investigated the selectivity of dopamine sensor in the presence of above mentioned molecules by using CV. It was observed that the other biomolecule did not show any obvious signal even in the presence of dopamine concentrations (Fig. 7d). There is no change in the peak potential and peak current of dopamine. Hence, the proposed Au NPs modified electrode was more suitable for selective and

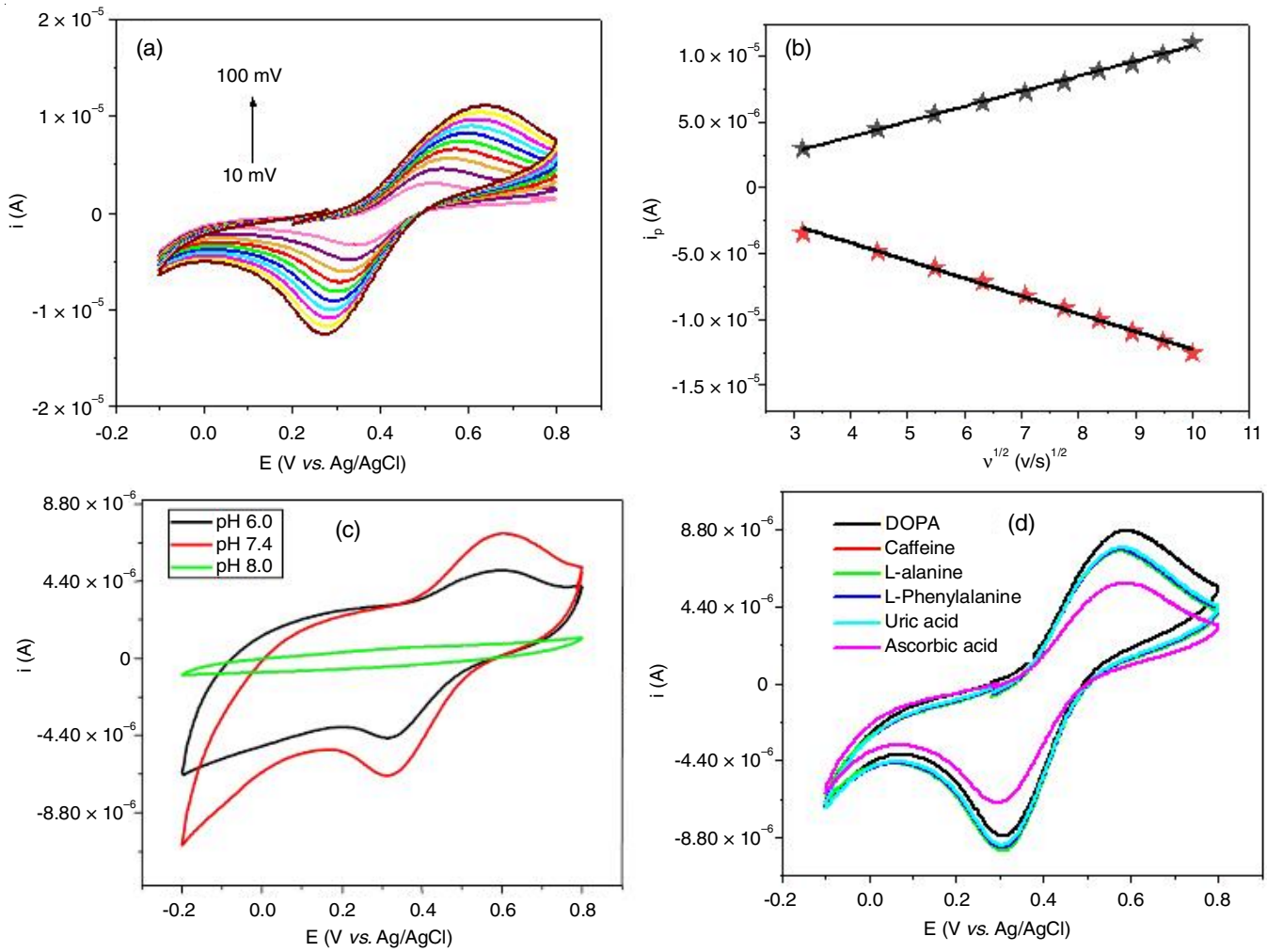

Fig. 7. (a) CV response for different scan rates from 10-100 mV/s using Au NPs modified electrode containing 39 nM dopamine in 0.1 M PBS; (b) Linear plot for scan rate *vs.* I_{pa} of dopamine (c) effect of different pH solutions (6, 7.4 and 8) using Au NPs modified electrode containing 39 nM dopamine in 0.1 M PBS and scan rate of 50mV/s; (d) interference study of Au NPs modified electrode in 0.1 M PBS at 50 mV/s with 39 nM dopamine in the presence of caffeine, L-alanine, L-phenylalanine, ascorbic acid, uric acid, respectively

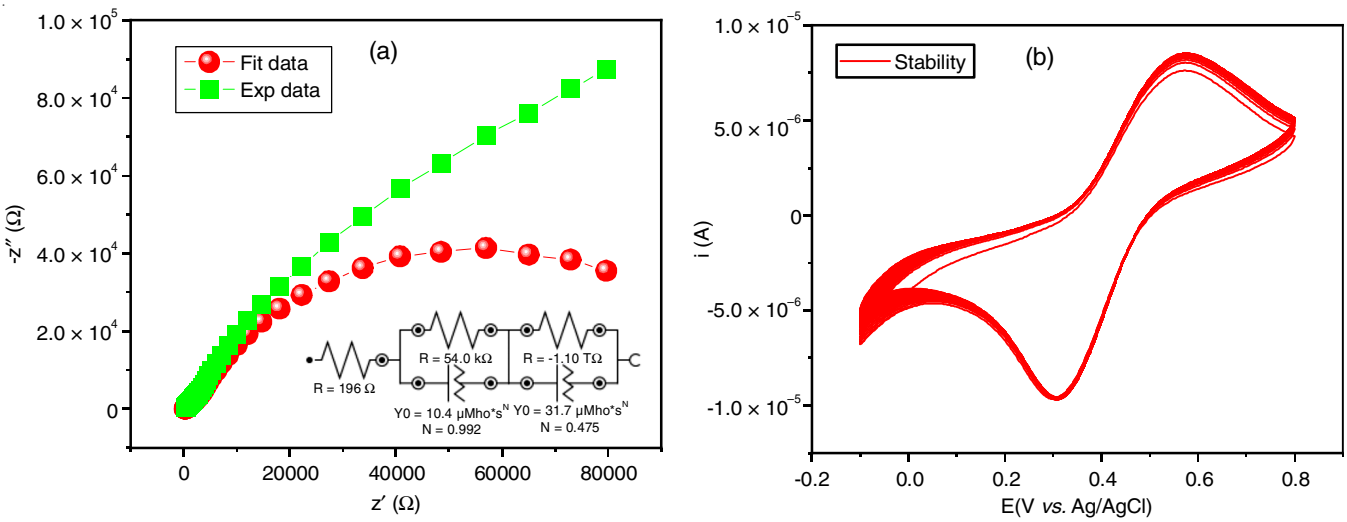

Fig. 8. (a) Typical Nyquist plot of electrode in 0.1 mM ferrocene at 0.6 V over Au NPs/GCE; (b) CV response of stability of modified electrode in 0.1 M PBS (pH 7.4) at 50 mV/s

high performance of dopamine sensor in presence of ascorbic acid, uric acid and amino acid.

Fig. 8a shows the Nyquist plot at potential of 0.6 V *vs.* Ag/AgCl, saturated KCl and the circuit model is represented in inset for Au NPs/GCE. The R_{ct} values obtained from modified electrode were 54 kΩ, respectively. The GCE exhibits larger semicircle having higher R_s value 196 Ω, revealing that faster electron transfer in modified electrode. The rapid electron transfer ascribed to excellent conductivity of Au NPs/GCE. The stability of Au NPs/GCE was studied by CV as shown in Fig. 8b. The storage stability of modified electrode was investigated and the oxidation peak current of dopamine was monitored by CV. Prior to analysis, the Au NPs modified electrode retains 97.8% of its initial response after 50 cycles.

Conclusion

Gold nanoparticles (Au NPs) were synthesized from the fresh pods of *Lablab purpureus* with particle size ranging between 10-15 nm with FCC crystal lattice. We have also successfully validated high sensitive detection of dopamine based on Au NPs modified electrode. The designed Au NPs modified electrode exhibits good reproducibility, high stability and favourable sensing performance for the detection of dopamine which is about 97.8%. Additionally, proposed novel sensor may be employed in the selective and simultaneous determination of dopamine and uric acid in their binary mixture. Thus, Au NPs modified electrode is possibly a promising candidate for the development of effective electrochemical sensors for the potential applications in medicine and biotechnology.

CONFLICT OF INTEREST

The authors declare that there is no conflict of interests regarding the publication of this article.

REFERENCES

1. X. Zhou, K. He, Y. Wang, H. Zheng and S.I. Suye, *Anal. Sci.*, **31**, 429 (2015); https://doi.org/10.2116/analsci.31.429
2. R.M. Wightman, L.J. May and A.C. Michael, *Anal. Chem.*, **60**, 769A (1988); https://doi.org/10.1021/ac00164a001
3. P. Damier, E.C. Hirsch, Y. Agid and A. Graybiel, *Brain*, **122**, 1437 (1999); https://doi.org/10.1093/brain/122.8.1437
4. J. Ping, J. Wu, Y. Wang and Y. Ying, *Biosens. Bioelectron.*, **34**, 70 (2012); https://doi.org/10.1016/j.bios.2012.01.016
5. I.D. Mandel, *J. Dent. Res.*, **66(1_suppl)**, 623 (1987); https://doi.org/10.1177/00220345870660S103
6. F. Wei, P. Patel, W. Liao, K. Chaudhry, L. Zhang, M. Arellano-Garcia, S. Hu, D. Elashoff, H. Zhou, S. Shukla, F. Shah, C.-M. Ho and D.T. Wong, *Clin. Cancer Res.*, **15**, 4446 (2009); https://doi.org/10.1158/1078-0432.CCR-09-0050
7. N. Wei, X.-E. Zhao, S. Zhu, Y. He, L. Zheng, G. Chen, J. You, S. Liu and Z. Liu, *Talanta*, **161**, 253 (2016); https://doi.org/10.1016/j.talanta.2016.08.036
8. Y. Zhang, S. Qi, Z. Liu, Y. Shi, W. Yue and C. Yi, *Mater. Sci. Eng. C*, **61**, 207 (2016); https://doi.org/10.1016/j.msec.2015.12.038
9. D. Rithesh Raj, S. Prasanth, T.V. Vineeshkumar and C. Sudarsanakumar, *Sens. Actuators B Chem.*, **224**, 600 (2016); https://doi.org/10.1016/j.snb.2015.10.106
10. B. Wang, Y. Chen, Y. Wu, B. Weng, Y. Liu and C. Li, *Mikrochim. Acta*, **183**, 2491 (2016); https://doi.org/10.1007/s00604-016-1885-5
11. X. Tian, C. Cheng, H. Yuan, J. Du, D. Xiao, S. Xie and M. Choi, *Talanta*, **93**, 79 (2012); https://doi.org/10.1016/j.talanta.2012.01.047
12. W. Li, L. Ding, Q. Wang and B. Su, *Analyst*, **139**, 3926 (2014); https://doi.org/10.1039/C4AN00605D
13. F. Figueredo, P. Garcia, E. Cortón and W. Coltro, *ACS Appl. Mater. Interfaces*, **8**, 11 (2016); https://doi.org/10.1021/acsami.5b10027
14. C. Sun, H. Lee, J. Yang and C. Wu, *Biosens. Bioelectron.*, **26**, 3450 (2011); https://doi.org/10.1016/j.bios.2011.01.023
15. H. Hassan, P. Sharma, M.R. Hasan, S. Singh, D. Thakur and J. Narang, *Mater. Sci. Energy Technol.*, **5**, 375 (2022); https://doi.org/10.1016/j.mset.2022.09.004
16. I. Hammami, N.M. Alabdallah, A. Al-Jomaa and M. Kamoun, *J. King Saud Univ.-Sci.*, **33**, 101560 (2021); https://doi.org/10.1016/j.jksus.2021.101560
17. P.K. Jain, K.S. Lee, I.H. El-Sayed and M.A. El-Sayed, *J. Phys. Chem. B*, **110**, 7238 (2006); https://doi.org/10.1021/jp057170o

18. P. Mulvaney, *Langmuir*, **12**, 788 (1996); https://doi.org/10.1021/la9502711
19. P. Elia, R. Zach, S. Hazan, S. Kolusheva, Z. Porat and Y. Zeiri, *Int. J. Nanomedicine*, **9**, 4007 (2014); https://doi.org/10.2147/IJN.S57343
20. M.J. Sweet, A. Chessher and I. Singleton, *Adv. Appl. Microbiol.*, **80**, 113 (2012); https://doi.org/10.1016/B978-0-12-394381-1.00005-2
21. G. Arun, M. Eyini and P. Gunasekaran, *Biotechnol. Bioprocess Eng.*, **19**, 1083 (2014); https://doi.org/10.1007/s12257-014-0071-z
22. M.R. Bindhu and M. Umadevi, *Mater. Lett.*, **120**, 122 (2014); https://doi.org/10.1016/j.matlet.2014.01.108
23. B. Ankamwar, *E-J. Chem.*, **7**, 1334 (2010); https://doi.org/10.1155/2010/745120
24. C.H. Foyer and S. Shigeoka, *Plant Physiol.*, **155**, 93 (2011); https://doi.org/10.1104/pp.110.166181
25. Y. Lu and L. Yeap Foo, *Phytochemistry*, **59**, 117 (2002); https://doi.org/10.1016/S0031-9422(01)00415-0
26. P. Mohanpuria, N. Rana and S. Yadav, *J. Nanopart. Res.*, **10**, 507 (2008); https://doi.org/10.1007/s11051-007-9275-x
27. C. Karuppiah, S. Palanisamy, S.-M. Chen, R. Emmanuel, K. Muthupandi and P. Prakash, *RSC Adv.*, **5**, 16284 (2015); https://doi.org/10.1039/C4RA14988B
28. L. Biao, S. Tan, Q. Meng, J. Gao, X. Zhang, Z. Liu and Y. Fu, *Nanomaterials*, **8**, 53 (2018); https://doi.org/10.3390/nano8010053
29. Y. Rao, G.K. Inwati and M. Singh, *Future Sci. OA*, **3**, FSO239 (2017); https://doi.org/10.4155/fsoa-2017-0062
30. S. Uthaman, H.S. Kim, V. Revuri, J.J. Min, Y.K. Lee, K.M. Huh and I.K. Park, *Carbohydr. Polym.*, **181**, 27 (2018); https://doi.org/10.1016/j.carbpol.2017.10.042
31. P. Zhang, F.H. Wu, G.C. Zhao and X.W. Wei, *Bioelectrochemistry*, **67**, 109 (2005); https://doi.org/10.1016/j.bioelechem.2004.12.004
32. B. Kamble, K. Garadkar, K. Sharma, P. Kamble, S. Tayade and B. Ajalkar, *Electrochem. Sci. Eng.*, **11**, 143 (2021); https://doi.org/10.5599/jese.956